A Periscope Detection Radar

Jeffrey J. Ousborne, Dale Griffith, and Rebecca W. Yuan

Detection of small cross-sectional periscopes with short, transient exposure periods requires a radar system with a sensitive detection threshold. Airborne radar detection systems were designed to provide such a capability in the open ocean. In littoral regions, however, these systems are manually intensive, and operators are overwhelmed by the numerous objects detected. The Automatic Radar Periscope Detection and Discrimination Program was implemented to automate the detection of transient periscope exposures while maintaining an extremely low false alarm rate. The approach incorporates a high-resolution radar with a two-stage periscope declaration process: conventional target detection with a moderate false alarm rate followed by signature discrimination to reduce the false alarms. Detected objects and persistent ocean clutter spikes are identified and eliminated by their spatial and temporal characteristics that differ from periscope signatures. This article discusses techniques used to achieve a sensitive detection threshold and resultant clutter spike false alarm rates. Theoretical analysis, radar data analysis, and radar emulation results are presented.
(Keywords: Antisubmarine warfare, Ocean clutter, Periscope, Radar.)

INTRODUCTION

Submarines operating in littoral regions routinely expose a variety of masts. Periscopes are raised for general safety sweeps, surveillance, and visual observation during torpedo attacks. Communication masts are raised to maintain command and control links, and snorkels are used when diesel electric submarines recharge their batteries. When a submarine exposes a mast, it is vulnerable to radar detection. Aircraft-based radar systems thus can detect all types of mast exposures.

The opportunity to detect periscopes was exploited in early radar experiments that prompted the development of the AN/APS-116 radar manufactured by Texas Instruments in the 1970s. The AN/APS-116 is an X-band, high-resolution, fast scanning system developed specifically to provide a periscope detection capability[1] on the carrier-based S-3 aircraft. The AN/APS-137 is an upgrade of this radar used primarily on the S-3; a limited number are also used on the land-based P-3 aircraft.

The primary enhancement incorporated into the AN/APS-137 was an inverse synthetic aperture radar capability for surface ship classification. Only minor modifications were made to the periscope detection mode during the upgrade. These radars successfully detect submarine mast exposures in the open-ocean environments for which they were designed. However, an alert operator must make the detection decision based on a radar PPI (plan position indicator) display. In littoral regions, the high density of small surface targets and debris quickly saturates the display and limits the operator's ability to detect transient mast exposures in the midst of numerous other targets.

The Automatic Radar Periscope Detection and Discrimination (ARPDD) Program[2] commenced in FY93 to demonstrate an automatic periscope detection capability for an airborne application and was later expanded to include the shipborne application. The program's primary goal is to detect very-short-duration transient periscope exposures with very low false alarm rates (FARs; one false alarm per mission for the airborne variant). The false alarm goal is particularly stringent since, within the ARPDD Program, a false alarm is any false periscope declaration; that is, a periscope declaration from any nonperiscope target such as a small boat is a false alarm. The joint target detection and FAR goal generates a stressing system performance requirement.

The ARPDD Program has three major development stages: breadboard, brassboard, and fleet demonstration unit (FDU). The breadboard phase successfully demonstrated a limited field-of-view automatic retrospective detector and also collected signature data for discrimination algorithm development and detector design enhancement. The brassboard system is under development and incorporates full-area coverage with real-time processing components for all elements of the design: automatic detection, direct discrimination, tracking, and indirect discrimination. The brassboard system is an engineering asset that includes both additional system capabilities and extensive data recording. Brassboard field testing will begin in 1997 in Kauai, Hawaii, followed by P-3 flight- and ship-based testing. The FDU system will incorporate all features deemed necessary to meet the performance requirement and will be designed for and tested by Fleet operators.

The Applied Physics Laboratory is a primary member of the ARPDD Program Team, which includes the Naval Research Laboratory, the Naval Air Warfare Center Weapons Division, and Texas Instruments. Texas Instruments is the prime contractor for the radar system. The Laboratory's responsibilities include technical design guidance, system design trade-off studies, and performance evaluations. As part of those responsibilities, APL has extensively analyzed the radar data and has developed a radar emulator to test the performance of design alternatives. The emulator provides a method to test design changes without incurring the time and cost impact of hardware development and additional field test evaluations.

A brief overview of the evolution in the radar design from the AN/APS-116 to the current ARPDD periscope detection approach is presented in the following sections. A theoretical and empirical performance analysis of the ARPDD is then discussed, followed by an evaluation of alternative detectors. Future plans for the ARPDD Program and APL tasks are also described.

RADAR DESIGN EVOLUTION

The AN/APS-116 and -137 radars use multiscan integration to detect small radar cross-section (RCS) objects in the periscope detection mode. This family of X-band radars has a 1-ft range resolution, 2.4° azimuthal beamwidth, 2000 pulses per second, and a 300-rpm scan rate in the periscope detection mode. High range resolution reduces the resolution cell size and thereby reduces the background clutter return. The fast scanning rate allows the system to integrate many scans of data during the detection process and thereby mitigates false alarms from background clutter that decorrelates quickly.

Range stretch techniques are used in the AN/APS-116 and -137 radars to achieve the scan-to-scan integration. Hardware bandwidth limitations existing at the time of development precluded the use of full-resolution detection. The range stretch process generates a first-threshold crossing if any cell in a 600-range-cell window crosses the first threshold. When this occurs, the location in the scan-to-scan integrator corresponding to that 600-range-cell window is updated with a threshold crossing. Multiscan integration is then applied in the scan-to-scan integrator. The range stretch approach also eliminates the need to compensate for target and platform motion since, during the integration period, the target typically remains in one 600-range-cell window. The approach also incurs a performance loss; however, it yields a significant improvement over lower range-resolution waveform detection processing.

The losses incurred by the AN/APS-116 and -137 range stretch technique are reduced in the ARPDD approach by implementing a detector at the full 1-ft range resolution. At this resolution the target velocity produces significant range movement during the multiscan detector integration period. For example, a 10-kt radial velocity target moves 85 ft in 5 s. A retrospective detector[3] identifies targets with possible range movement. This two-threshold binary detector technique applies an M of N detection criterion within velocity templates that cover the range of possible target velocity vectors in N scans of data. Each velocity

template has a range/scan relationship that corresponds to a possible target velocity. Some integration losses still occur because each template typically has several range-resolution cells in each scan. When any resolution cell within a velocity template exceeds the first threshold during a scan, the entire scan exceeds the first threshold. If *M* of the *N* scans in the template exceed the first threshold, a second threshold is exceeded and a detection is declared. The ARPDD implementation fixes *N* at 25 scans, corresponding to 5 s of data with the antenna scanning at 300 rpm.

In contrast to the range stretch technique, retrospective detection with 1-ft range-resolution data requires the platform motion to be compensated to better than the 1-ft range-resolution cell during the integration period. Data from the Global Positioning System and an inertial measurement unit are used in a Kalman filter algorithm to compensate the radar data before detection processing.

The detection sensitivity required to reliably detect submarine masts also results in the detection of many persistent clutter spikes and small targets found in littoral regions. A clutter spike refers to the radar energy returned from ocean surface features that is larger than the return energy from the surrounding area. This increased return energy is frequently associated with breaking waves and can persist for several seconds. In addition to large-amplitude clutter spikes, objects such as small boats, fishing and marker buoys, debris, etc., also have sufficient RCS to be detected.

To achieve the ARPDD performance goal, the system concept combines both conventional and unique designs. Conventional radar detection and tracking are used along with special automatic discrimination methods. Discrimination is required to achieve good detection sensitivity while maintaining a very low false periscope declaration rate.

The first phase of the ARPDD Program focused on building a test radar system, i.e., the breadboard radar, and collecting data with it. This system was used in 1994 to evaluate automatic retrospective detector performance, validate the motion compensation algorithm, validate target discrimination feasibility, and collect data to enhance the detector design and develop discrimination algorithms.

The breadboard radar comprises the Naval Research Laboratory prototype APS-137 radar host, a limited-coverage automatic detector prototype, and data recorders. Implementation of the breadboard retrospective detector incorporates a first-threshold automatic gain control (AGC), which is similar to the AN/APS-137 AGC, and a second threshold implemented with seven velocity templates covering ±15-kt target speeds. Two digital recording media capture data for post-test analysis. A high-bandwidth (4 Mbytes/s, 5-Gbyte capacity) very large data storage (VLDS) recorder captures the raw radar data. The 1-ft range-resolution data are recorded as 8-bit in-phase and quadrature samples. When the antenna is scanning at 300 rpm, data are recorded in a region typically 3 nmi in range by 18° (20 pulses) in azimuth. Data can also be collected with the antenna fixed in azimuth or locked onto a target. In this "spotlight" mode, data are obtained over a 512-ft range extent in one azimuthal location at 2000 pulses per second. A lower-bandwidth 8-mm tape drive (0.5 Mbyte/s, 4.5-Gbyte capacity) is used to capture the retrospective detector output. Analysis presented later in this article uses breadboard data.

The second radar development product of the ARPDD Program is called the brassboard radar system. This system extends the limited-coverage breadboard retrospective processor to full-area coverage and incorporates all other elements of the baseline ARPDD approach. The system includes a radar RF/IF section, an automatic detector, an automatic discriminator, a tracker, and an indirect discriminator. A simplified system block diagram is shown in Fig. 1, and its components are described in the following paragraphs.

An APS-137 RF/IF with a new receiver–exciter–synchronizer provides the front end of the brassboard system. The RF/IF raw data are processed through two detection channels and one discrimination channel. (The output of these three channels is then processed by the indirect discriminator.) One detection channel, the slow-target automatic detector (STAD), includes a first-threshold logarithmic detector incorporating a constant false alarm rate (log-CFAR) controller followed by a retrospective filter. The second channel, the fast-target automatic detector (FTAD), includes a first-threshold logarithmic detector incorporating a fast time constant controller followed by a retrospective filter. The STAD is optimized to detect slow-moving submarine masts since submarine speeds are limited when masts are exposed. The FTAD must maintain tracks on fast targets not routinely detected by the STAD. These targets are tracked so that when they are occasionally detected by the STAD, they are correctly associated with a fast target and not incorrectly identified as a transient mast exposure. (Fast targets are occasionally detected in the STAD when target range extent or changes in target velocity produce sufficient threshold crossings in the STAD velocity templates.)

The brassboard STAD design includes a two-threshold retrospective filter like the breadboard. However, the first threshold is a log-CFAR peak-pick threshold in contrast to the breadboard AGC. (The peak-pick threshold defines the sample with the largest amplitude return in the specific range gate as the one and only sample that exceeds the threshold.) The log-CFAR reduces the system's sensitivity to extended features such as clutter and large targets, and the peak-pick range gate guarantees a constant first-threshold

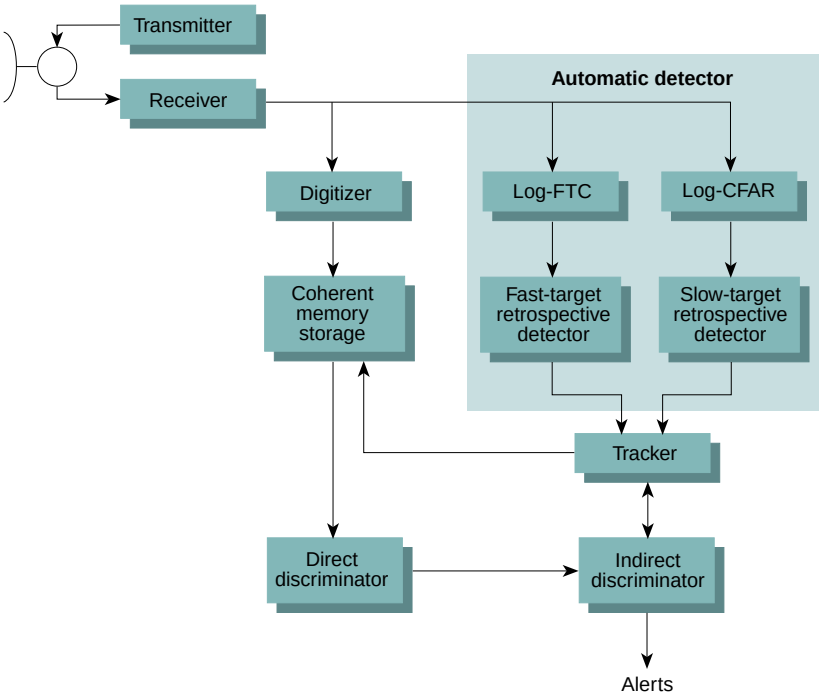

Figure 1. Block diagram of the Automatic Radar Periscope Detection and Discrimination Program radar system design (FTC = fast time constant, CFAR = constant false alarm rate).

FAR. The log-CFAR is a logarithmic receiver followed by a sliding window average-subtracted from the return signal. The second STAD threshold is a retrospective detector implemented with a variable *M* value, fixed *N* value of 25 scans, and 31 velocity templates covering ±15-kt target speeds. Longer STAD integration times can also be evaluated in real time with a fixed *N*=25 by reducing the antenna rotation rate. The brassboard provides antenna scanning rates of 300 (nominal), 240, and 210 rpm, which yield integration times of roughly 5, 6, and 7 s, respectively.

The brassboard tracker processes the STAD and FTAD detections and enables the system to link events over time. The tracker maintains tracks on all persistent targets and determines if a new detection is associated with an existing track or is a new target (e.g., a transient periscope or sea spike). The indirect discriminator makes the final periscope detection declaration. It uses the tracker associations to combine multiple direct discrimination results to reduce false target declarations when the targets are detected and tracked for extended periods. This reduces the probability of false alarms (PFAs) from targets that may occasionally be erroneously identified by the direct discriminator as a submarine mast.

Discrimination processing is required to differentiate periscope detections from other hard targets and clutter. The direct discrimination channel includes an analog-to-digital converter, an 8-Gbyte coherent memory, signature extraction algorithms, and a direct discriminator. The coherent memory is used to store the last 7 s of radar data. When an STAD detection occurs and the indirect discriminator determines that it is a possible periscope signature, the 25 scans (5 s) by 128 ft of radar data that generated the detection are extracted from the coherent memory and sent to the direct discriminator. The direct discriminator determines if it is a submarine mast, other small target, or clutter spike signature (D. Reade, personal communication, 13 Sep 1995). The 1-ft range resolution is a critical enabling element of this discrimination process since range structure provides an obvious discrimination feature for hard targets. The accuracy of clutter spike discrimination is critical to meeting the stringent system FAR goal while maintaining detection sensitivity. The direct discriminator uses signature features like range extent, linearity, range profile cross correlation, and amplitude distribution to differentiate mast targets from clutter spikes.

The brassboard radar is an engineering asset with significant flexibility. It will be used to determine individual element and total system performance as well as performance sensitivities to a variety of system parameters. Several data recorders will capture information for off-line analysis. Three VLDS recorders will simultaneously record raw radar data, first-threshold crossing data, and signatures sent to the direct discriminator. In addition, seven 8-mm tape drives will record radar status and navigation data as well as outputs from the detector, tracker, direct discriminator, indirect discriminator, etc. These data will be used in near–real time to assess system performance and in posttest analysis.

The third radar development phase of the ARPDD Program will incorporate all features necessary to meet the system performance goal within the FDU system, which, again, is designed to be operated by Fleet personnel and will demonstrate the operational utility of the system. Several capabilities beyond the ARPDD baseline concept (e.g., amplitude integration in the STAD retrospective detector, dual-polarization detection and discrimination, and Doppler target discrimination) are being considered for the FDU if the baseline concept does not achieve the performance goal during brassboard testing.

ARPDD PERFORMANCE ANALYSIS

The implementation of the retrospective detector in the ARPDD approach offers a potentially significant enhancement in detection sensitivity over that achieved in the AN/APS-116 and -137 radars. The improvement has been theoretically estimated. Figure 2 shows the relative first-threshold level required to maintain a specific detector output FAR. This computation assumes a clutter-limited system with an uncorrelated, lognormally distributed clutter having a 9-dB log standard deviation. Such a long-tailed distribution is frequently used to represent high-resolution radar clutter like that observed with the 1-ft AN/APS-137. A 13 of 25 *M* of *N* retrospective detector represents the ARPDD STAD design with 7 to 63 velocity templates covering ±15-kt target speeds. Under these conditions a retrospective detector with 31 velocity templates has a 13-dB lower detection threshold than the AN/APS-116 and -137 range stretch technique. In a noise-limited condition with an uncorrelated "Rayleigh" distribution, this improvement is much smaller, about 3 dB (not shown). As discussed later, the clutter background is not uncorrelated as assumed in this theoretical computation. Although the actual gain achieved with the retrospective filter is less than this theoretical computation, it is still significant.

System detection sensitivity is maintained by operating at a high first-threshold PFA, for example, 0.004, corresponding to one threshold crossing every 256 ft on each pulse. Although a high first-threshold FAR is produced, detector output FARs are reduced to 10^{-12} (1 per day) in uncorrelated noise and uncorrelated clutter using a 13 of 25 detector. The resultant system sensitivity was theoretically evaluated using an empirical model for the mean ocean clutter[4] and a lognormal clutter distribution with a log standard deviation determined by the radar-resolution cell size. Figure 3 shows the theoretical first-threshold RCS sensitivity as a function of sea state and range when the antenna is pointed upwind. At the longer ranges, beyond the point where the curves converge, the system is noise-limited. Changes in the first-threshold PFA or changes in the clutter distribution affect this detection sensitivity.

Scan-to-scan correlation in the clutter background increases the FAR of the clutter spikes. As expected, the number of spikes detected is many orders of magnitude greater than predicted for uncorrelated clutter. The breadboard real-time detection results highlighted numerous occurrences of ocean clutter spikes that persisted for many seconds. The large data sets collected with the breadboard system were used in posttest analysis to characterize these persistent spikes. A sample clutter spike detected by the retrospective processor is shown in Fig. 4. It is moving at roughly 9 kt inbound (15 ft in 5 s) and is wide (>10 ft) during most of its existence. The clatter spike also exhibits erratic

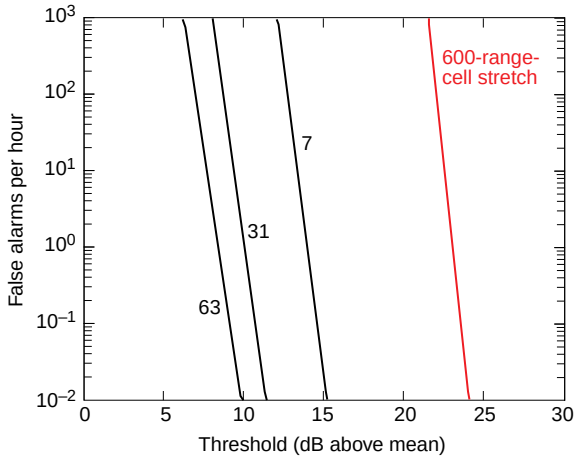

Figure 2. Theoretical performance benefit of the full-resolution automatic detector with 7, 31, and 63 velocity templates (black lines) and range stretch detector (red line). Background interference is assumed to be uncorrelated from scan to scan. (*M* of *N* = 13 of 25; clutter standard deviation = 9 dB.)

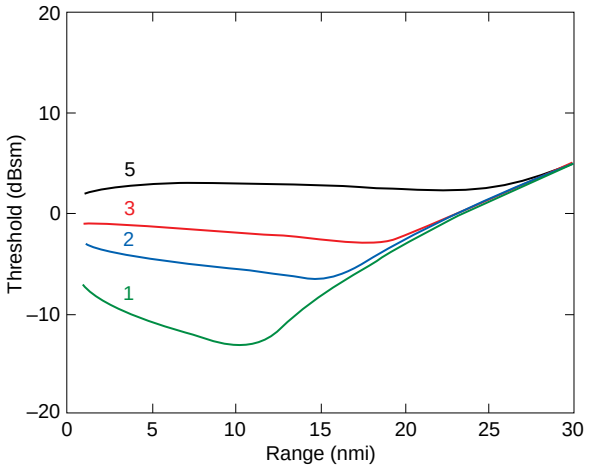

Figure 3. Theoretical first-threshold radar cross-section detection sensitivity for sea states 5, 3, 2, and 1. Platform height = 1000 ft; first-threshold false alarm rate = 0.004.

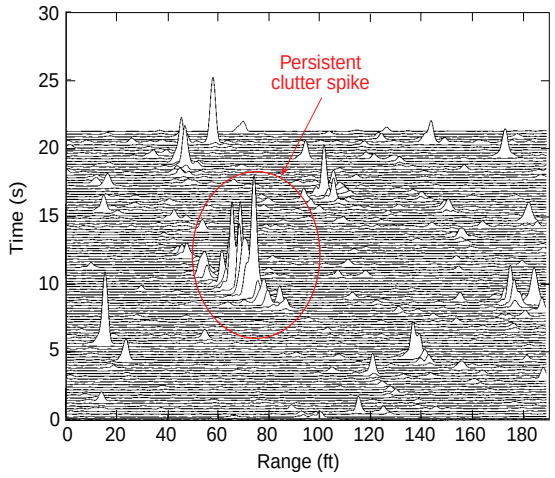

Figure 4. The radar signature of a persistent clutter spike.

features, i.e., its range extent and amplitude changed significantly over its lifetime.

Breadboard radar data were analyzed in a three-step procedure to determine the frequency of clutter spikes as a function of clutter spike duration. First, an amplitude threshold was set to identify all returns that exceeded that threshold. The thresholds were set to achieve a specified PFA of 0.01 or 0.001 (the ARPDD baseline design allows the adjustment of the first-threshold PFA between these values). Second, the clutter spike events were tracked in range. A tracker is required since the clutter spikes move quickly through the 1-ft range-resolution cell. Sample histograms of clutter spike velocities detected by a retrospective processor are shown in Fig. 5 for an upwind and crosswind look direction. These persistent spikes typically travel in the direction of the seas/winds, and apparent speed is a function of radar orientation. Note that an azimuth tracker is not required. Azimuth beamwidths are large, for example, 1000 ft at 4 nmi. Typical clutter spikes traverse a small fraction of that distance in their lifetime. The final step in the clutter spike duration analysis computes the time between the initialization and termination of the clutter spike track. The number of clutter spikes for a specific duration is normalized to the number of spikes that occur each second in each radar-resolution cell.

Sample clutter spike persistence is shown in Fig. 6. Each curve represents the data from one 25-min data collection run. The number of clutter spikes decreases by roughly an order of magnitude for each second of increase in duration. Long integration times could be applied to mitigate the clutter spike problem; however, their use also reduces the detectability of short-duration transient submarine mast exposures. The number of persistent clutter spikes is also a function of the detection threshold. Data indicate that reducing the first-threshold FAR by a factor of 2 reduces the number of persistent spikes by more than an order of magnitude. However, reductions in the first-threshold FAR increase the RCS detection threshold.

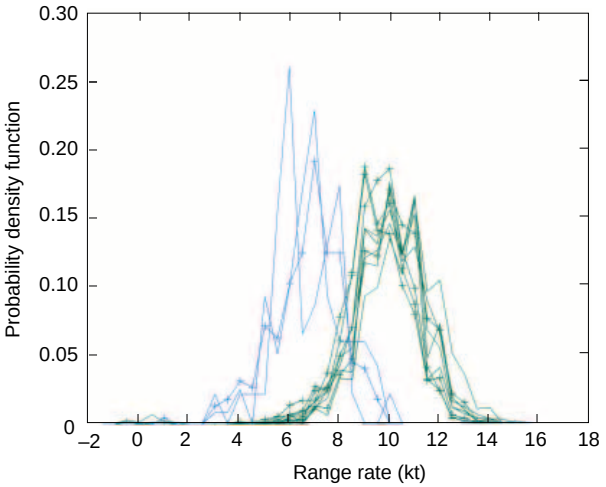

Figure 5. Velocity histograms of persistent clutter spikes from an emulated brassboard design for upwind (green) and crosswind (blue) directions. These data were collected from a 100-ft site under sea state 5 conditions at 5 to 8 nmi. Curves with + are vertical polarizations; those without are horizontal polarizations.

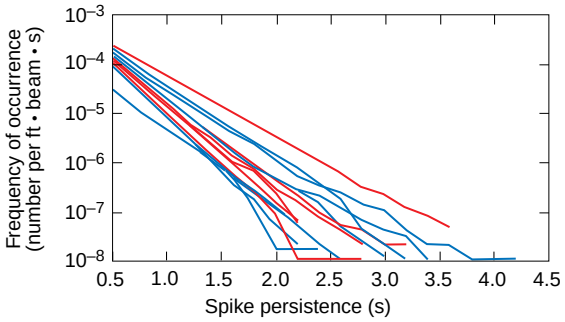

Figure 6. The frequency of occurrence of persistent clutter spikes as a function of the spike duration. Data have been normalized to the number of spikes per resolution cell per second (red and blue = horizontal and vertical polarization, respectively; first-threshold FAR = 0.001).

RADAR DETECTOR DESIGN EVALUATIONS

A radar emulator was developed in software to evaluate the performance of several STAD and FTAD detector designs. The emulator processes the recorded raw radar data through a software version of the STAD or FTAD and outputs detection and false alarm results. This emulation allows new design concepts to be evaluated before committing the time and funding required to build and field test the hardware implementation of the design concept.

Using emulation studies and breadboard data, alternative brassboard STAD implementations were evaluated. Emulation was used to test the log-CFAR concept. Log-CFAR filter widths of 21 to 51 ft were assessed. The log-CFAR filter can include a guard band that excludes several cells around the center of the filter. Guard band extents from 0 to 5 range cells were tested. Shorter-length log-CFAR filters remove more of the shorter range extent features. The "optimal" filter length is a function of the range structure of the target and features that create false alarms. The emulator was also used to test the peak-pick first-threshold concept. Peak-pick range gates of 125 to 1000 ft were evaluated, corresponding to first-threshold PFAs of 0.008 to 0.001, respectively. Longer peak-pick range gates reduce the FAR at the expense of detection sensitivity.

The emulator was also used to test M value sensitivity. M values ranging from 8 to 21 were examined. The "optimal" M value is a function of the target correlation and correlation of the persistent clutter

spikes that produce false alarms. Large M values decrease false alarms from correlated background features, but they also reduce target detection performance.

Figure 7 shows emulator outputs for four different STAD designs. Figure 7a was created with the original breadboard AGC design and a 13 of 25 retrospective filter with 7 velocity templates; Fig. 7b was created with the same design as 7a but incorporated 31 velocity templates; Fig. 7c was created by replacing the original AGC with a peak-pick first threshold; and Fig. 7d was created by replacing the original AGC with a log-CFAR and peak-pick first threshold. The log-CFAR filter is 21 ft long with a 3-ft guard band. Figures 7a through 7d represent the same 22 min of data from a 3 nmi by 18° region. Each dot represents a STAD detection. Two targets are present, a spar buoy at roughly 3.3 nmi and a support ship at roughly 4.4 nmi. Other detections are generated by ocean clutter. As seen, the original design has many clutter spike detections. The log-CFAR design substantially reduces clutter spike detections while maintaining or improving spar buoy detectability. Large range extent features like ships (upper right-hand corner of Figs. 7a through 7c) are less detectable since the log-CFAR removes such features. The log-CFAR design always improved spar buoy detection/clutter spike false alarm performance. However, the degree of improvement over the emulated breadboard design depended on environmental conditions and geometry.

One option being considered for the FDU design has been tested with the emulator. This option includes amplitude integration in the STAD retrospective detector. One possible amplitude integration implementation approach sets an amplitude threshold for the mean target amplitude in the 25 scans in addition to a binary M of N threshold in each velocity template. Figure 8 shows an example of emulator results. The number of target detections and false alarms is normalized by the emulated breadboard results. Each curve represents a different M value (8 to 12) in the binary M of N threshold, and each symbol on the curves represents a different amplitude threshold. The best performance occurs in the upper left-hand corner of the plot (i.e., high target detectability and low FARs). For example, the amplitude detector with an M of 10 has a higher target detection performance and fewer false alarms than the 12 of 25 binary detector. Note that the implementation of an amplitude integration technique

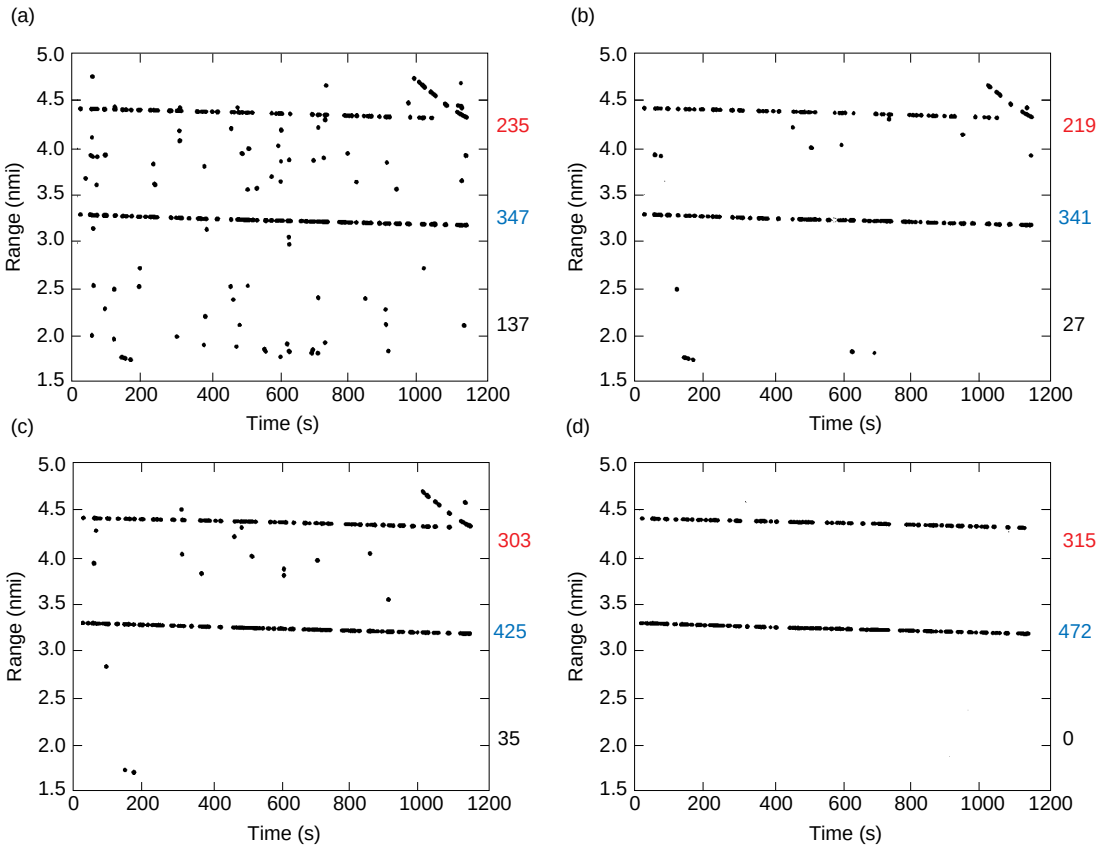

Figure 7. Emulated detector outputs for several detector designs: (a) breadboard design, (b) breadboard design, but with the number of velocity templates increased from 7 to 31, (c) peak-pick first threshold, and (d) log-CFAR and peak-pick first threshold. Each dot represents a detection by a slow-target automatic detector. (Red numbers on right axes denote number of boat detections, blue denote number of spar detections, and black denote clutter detections.)

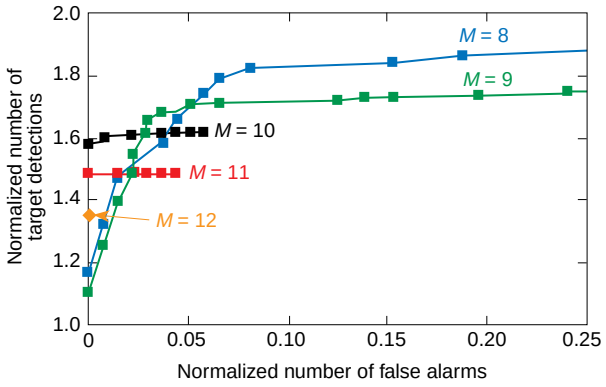

Figure 8. Emulated amplitude detection performance. The number of target detections and false alarms is normalized by the emulated breadboard results. *M* values of 8 to 12 are shown. Each symbol on the curves represents a different amplitude threshold. A 21-ft-long log-CFAR filter is followed by the peak-pick first threshold and a retrospective filter with 31 velocity templates.

requires a method to automatically set an amplitude threshold. These results do not reflect losses that are associated with the determination of this threshold.

THE FUTURE OF THE ARPDD PROGRAM

Texas Instruments is currently fabricating the brassboard system for the ARPDD Program. System performance testing is planned in three phases: (1) at low- and high-elevation shore sites corresponding to ship and aircraft elevations, (2) with the Naval Research Laboratory P-3 aircraft, and (3) with a DD-963–class destroyer. Shore site testing is scheduled to start in 1997. Test objectives are to measure the brassboard performance, define the "best" FDU system configuration, and estimate FDU performance.

The Applied Physics Laboratory has five responsibilities associated with the brassboard tests.

1. Develop on-site analysis software to assess system performance by analyzing the outputs from each radar element
2. Enhance the radar emulator to evaluate the benefits of dual-polarization data
3. Assess the motion compensation system
4. Develop and field a remotely controlled and instrumented telescoping spar buoy
5. Collect and analyze environmental data during the tests

The telescoping spar buoy will be used as a reference target during the tests to assess system detection sensitivity. The brassboard dual-polarization capability will serve to identify the best single polarization and the potential benefits of scan-to-scan or pulse-to-pulse polarization switching. Scan-to-scan polarization diversity performance will be measured in near–real time during shore tests; pulse-to-pulse polarization diversity performance will be evaluated with posttest emulation.

The brassboard Doppler data collection capability will be used to evaluate the performance of Doppler discrimination. Features that are difficult to discriminate with the scanning mode data can typically be discriminated by processing Doppler signature data collected in a spotlight mode. Submarine masts are identified by their narrow Doppler bandwidth and smooth perturbations in the Doppler center frequency. In contrast, small floating objects like buoys show rapid fluctuation in the Doppler center frequency as the waves move the target around. Doppler signatures can be provided in the FDU system by a cued second aperture or by stopping a scanning antenna and dwelling the antenna for several seconds on the target.

SUMMARY

Radar data analysis and radar design emulation results were used to identify and evaluate an automatic detector capable of achieving the sensitivity required to detect short-duration transient periscope exposures. This detection sensitivity also results in the detection of numerous persistent clutter spikes. The quantities and characteristics of the persistent clutter spikes were evaluated as a function of the environment and detector design. Preliminary results indicate that the direct discriminator—the second stage of the two-stage declaration process—provides sufficient clutter spike discrimination to achieve the system performance goal. Field tests in 1997 will be conducted to validate those findings.

REFERENCES

[1] Smith, J. M., and Logan, R. H., "AN/APS-116 Periscope Detecting Radar," *IEEE Trans. Aerosp. Electron. Sys.* **AES-16**(1), 66–73 (Jan 1980).
[2] *Airborne Radar Automatic Periscope Detection and Discrimination Enhanced ATD Execution Plan*, NAVAIR PMA-264, Naval Air Systems Command, Washington, DC (30 Aug 1993).
[3] Prengaman, R. J., Thurber, R. E., and Bath, W. G., "A Retrospective Detection Algorithm for Extraction of Weak Targets in Clutter and Interference Environments," in *Proc. IEEE EASCON '83*, pp. 153–157 (Sep 1983).
[4] Sittrop, H., "On the Sea-Clutter Dependence on Wind Speed," in *Proc. IEE International Conf.* **Radar-77**, pp. 110–114 (25–28 Oct 1977).

THE AUTHORS

JEFFREY J. OUSBORNE received his M.S. degree in electrical engineering from The Johns Hopkins University G.W.C. Whiting School of Engineering and a B.S.E.E. degree from the University of Maryland. He has worked at APL in radar, acoustics, and communications systems analysis as well as field-test data analysis and interpretation. His recent experience includes system performance analysis of a radar system for air and ship platforms for the ARPDD Program. Mr. Ousborne is the project manager for that effort and Assistant Group Supervisor of APL's Signal and Information Processing Group. His e-mail address is Jeffrey.Ousborne@jhuapl.edu.

DALE GRIFFITH received B.S. and M.S. degrees in electrical engineering from Michigan State University in 1985 and 1988, respectively. He joined the Submarine Technology Department's Systems Group in 1986. While at APL, he has focused on signal processing as applied to synthetic aperture radar, sonar, and conventional radar. His e-mail address is Dale.Griffith@jhuapl.edu.

REBECCA WEN-LING YUAN joined APL in 1991 after receiving her M.S.E.E. degree from the University of Houston. She is a member of the Signal and Information Processing Group in the Submarine Technology Department. Her past assignments mainly involved the application of signal detection and estimation theory for target detection and tracking using acoustic sensors. Ms. Yuan is now working on the ARPDD Program where she has developed the emulation software for analyzing and evaluating the performance of a baseline automatic detector as well as other alternative design concepts. Her e-mail address is Becky.Yuan@jhuapl.edu.